

Accepted Manuscript

Research papers

Impact of storm tides and inundation frequency on water table salinity and vegetation on a juvenile barrier island

Tobias Holt, Stephan Seibert, Janek Greskowiak, Holger Freund, Gudrun Massmann

PII: S0022-1694(17)30614-5

DOI: <http://dx.doi.org/10.1016/j.jhydrol.2017.09.014>

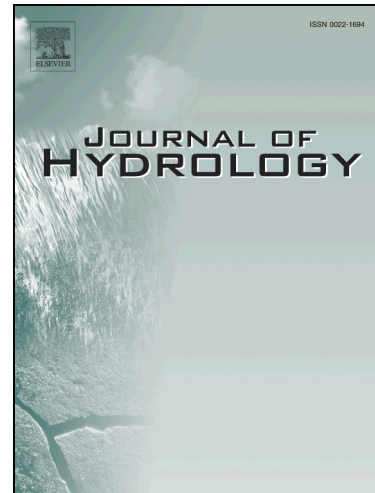
Reference: HYDROL 22234

To appear in: *Journal of Hydrology*

Received Date: 4 May 2017

Revised Date: 6 September 2017

Accepted Date: 7 September 2017



Please cite this article as: Holt, T., Seibert, S., Greskowiak, J., Freund, H., Massmann, G., Impact of storm tides and inundation frequency on water table salinity and vegetation on a juvenile barrier island, *Journal of Hydrology* (2017), doi: <http://dx.doi.org/10.1016/j.jhydrol.2017.09.014>

This is a PDF file of an unedited manuscript that has been accepted for publication. As a service to our customers we are providing this early version of the manuscript. The manuscript will undergo copyediting, typesetting, and review of the resulting proof before it is published in its final form. Please note that during the production process errors may be discovered which could affect the content, and all legal disclaimers that apply to the journal pertain.

**Impact of storm tides and inundation frequency on water table salinity and vegetation
on a juvenile barrier island**

Tobias Holt^{a*}, Stephan Seibert^a, Janek Greskowiak^a, Holger Freund^b, Gudrun Massmann^a

^aInstitute for Biology and Environmental Sciences, Carl von Ossietzky-University, Ammerländer Heerstraße 114-118, D-26129 Oldenburg, Germany

^bInstitute for Chemistry and Biology of the Marine Environment, Carl von Ossietzky-University, Schleusenstraße 1, D-26382 Wilhelmshaven, Germany

*Corresponding author: tobias.holt@uni-oldenburg.de (T. Holt)

Abstract

Freshwater lenses are generally of major interest for drinking water supply in coastal environments. Knowledge of the interrelations between ground surface elevation, sea level, inundation frequency, groundwater salinity and vegetation is also vital to understand coastal ecosystem functioning. This study provides an integrated analysis of these parameters at a barrier island in the North Sea that is currently developing under highly dynamic processes, but remains largely unaffected by humans. This study is particularly relevant in view of predicted sea-level rise and increasing storm frequencies, as the analysis of groundwater salinities at the water table, water level data and ground surface elevation reveal the pronounced influence of storm tides and inundation frequency on the water table salinity at the eastern part of the barrier island Spiekeroog, the so-called ‘Ostplate’, located off the northwest coast of Germany. The shallow freshwater is restricted to the elevated dune areas and shows spatial and temporal variations, depending on the time passed since the last storm tide. The water table salinities depend on inundation frequencies, whereby more than three flooding events in the year prior to sampling led to brackish water table salinities. Inundation frequency and water table salinity are both largely a function of ground surface elevation, and the dependence of water table salinity on the ground surface elevation can be quantified with an exponential function. Combining this function with digital elevation models enables the extrapolation and reconstruction of present and past water table salinity

distributions within the study area, which overall show decreasing salinities with increasing ground surface elevation. Since the vegetation zonation also depends on the inundation frequency, an identified match between water table salinities and vegetation zones suggests that water table salinities may be inferred from vegetation maps in the future.

Keywords: coastal aquifer, morphodynamics, vegetation zonation, sea-level rise, ground surface elevation, groundwater salinization

1. Introduction

Coastal aquifers are highly vulnerable to salinization, in particular in view of rising sea levels, increasing storm frequency and potential overuse (Post, 2005). Below barrier islands, a freshwater body typically forms by precipitation infiltrating into the highly permeable sediments, mainly below dune areas (elevated areas), which are not prone to inundation. Due to differences in density, a so-called freshwater lens develops that floats on top of the underlying saltwater (e.g. Collins and Easley, 1999; Fetter, 1972; Vacher, 1988; Vandenbohede and Lebbe, 2007). The resulting transition zone, i.e. the freshwater-saltwater interface, is normally not a sharp interface, but a dynamic boundary or mixing zone (Anderson and Lauer, 2008; Collins and Easley, 1999; Stuyfzand, 1993). In tidal systems, freshwater discharge occurs near the low water line and is restricted by circulating saltwater from above ('upper saline plume') and below ('saltwater wedge'; Robinson et al., 2007). The freshwater lens and its transition zone are influenced by both natural and anthropogenic factors (Anderson and Lauer, 2008; Schneider and Kruse, 2006). Natural factors are island stratigraphy, vegetation patterns, seasonal changes in recharge/discharge, ground elevation and tidal effects (e.g. Anderson and Lauer, 2008; Schneider and Kruse, 2006). Anthropogenic factors are saltwater intrusion as a consequence of overextraction and contamination from surface sources (e.g. Schneider and Kruse, 2006; White et al., 2007; White and Falkland, 2010). In the absence of coastal protection measures such as dykes, freshwater salinization can also be caused by inundation and overwash events (Anderson, 2002; White et al., 2007). As a characteristic of coastal areas around the world, the

inundation by seawater during storm tides can lead to strong salinization of the shallow freshwater (Gingerich et al., 2017; Klassen and Allen, 2017; Post and Houben, 2017; Terry and Falkland, 2009; Werner et al., 2013). The recovery of the former freshwater regions of coastal aquifers after inundation is due to recharge from rainwater, and may take several months (Terry and Falkland, 2009). According to findings of Houben et al. (2014), on the barrier island Langeoog, west of Spiekeroog, recharge rates depend on land use and topography, whereby the highest rates occur in the dune valleys, representing the main source of recharge. Anderson (2002) and Yang et al. (2013) reported that recovery time can also take years until salinities suitable for drinking water are reached. Post and Houben (2017) showed that freshening of the main freshwater lens to pre-inundation levels took four years on the near-by island of Baltrum, following a devastating storm tide in 1962.

Barrier islands are naturally characterized by a low topography, and physical parameters such as elevation above sea level and distance from the shoreline determine the inundation frequency. Hence, they are highly sensitive to changes in sea level and frequency of storm tides. This is of particular relevance since the sea level is predicted to rise and associated storm activities are to potentially increase in the future as a consequence of climate change (IPCC, 2007; Wolner et al., 2013).

Ground surface elevation also strongly influences the presence of ecosystems like salt marshes on the back-barrier shores of barrier islands. Several studies from different regions worldwide have shown that elevation and corresponding inundation frequencies and durations as well as salinity levels create a complex gradient network determining salt marsh vegetation and zonation patterns (e.g. Bockelmann et al., 2002; Erchinger, 1985; Sánchez et al., 1996; Silvestri et al., 2005; Suchrow and Jensen, 2010). Most studies investigating vegetation distribution in salt marshes refer to soil salinity, though Bockelmann and Neuhaus (1999) have also suggested that soil salinity is strongly associated with groundwater salinity, decreasing from the lower to the upper salt marsh.

The study area, the so-called ‘Ostplate’, is located at the eastern part of Spiekeroog, which is a barrier island in the North Sea belonging to the East Frisian Island chain. The

Ostplate evolved from a sand bar to a juvenile barrier island within the last 80 years and although connected to the older western part of Spiekeroog, the Ostplate forms an entirely separate landscape. According to preliminary investigations by Röper et al. (2013), freshwater is present below the current dune ridge but is presently not used for the island's drinking water supply, which is provided from a large freshwater lens below the older western part of Spiekeroog. Similar to the freshwater resources of other barrier islands, the freshwater lens of Spiekeroog is prone to erosion, flooding through storm tides and potential impacts of predicted sea-level rise. However, simulation results by Sulzbacher et al. (2012) suggest that the general shape of the freshwater lens of near-by Borkum will not experience essential changes following sea-level rise until 2100. The Ostplate is well-protected due to nature conservation requirements and, being located in the national park 'Nationalpark Niedersächsisches Wattenmeer' and thus part of the World Heritage Site 'Wadden Sea' (declared in 2009), remains largely unaffected by humans. Hence, the island is not only an ideal field site to study the evolution of a new freshwater lens in a highly morphodynamic environment, but also to research the impacts of inundation frequency and storm tides under natural conditions (i.e. without coastal protection measures) on water table salinities and the local vegetation.

The aims of this study were i) to investigate the spatial extent of the shallow freshwater at different times of the year (i.e. prior to and after the winter storm-flood season), ii) to infer the time it takes to refresh the shallow groundwater after flooding with saltwater, iii) to assess and quantify the influence of ground surface elevation and inundation frequency on the shallow groundwater salinities (in the following referred to as water table salinities) and vegetation zonation, and iv) to relate ground surface elevation to water table salinity based on a derived empirical equation that can be used for water table salinity reconstruction and predictions.

2. Study area

Spiekeroog is part of the East Frisian Island chain off the northwest coastline of Germany and lies between the islands of Langeoog to the west and Wangerooge to the east (Fig. 1). The distance between the island and the mainland is approximately 6.5 km. The present island stretches ~9.8 km in west-east direction, from the Otzumer inlet (to the west) to the Harle inlet (to the east). The western part of the island (~4.5 km) is inhabited whereas the remaining ~5.3 km encompass the Ostplate, which is younger, highly protected and uninhabited. Spiekeroog has a maximum width of approximately 2.3 km (north-south extent) and a total area of about 21.3 km² (Petersen and Pott, 2005; Streif, 1990).

Fig. 1

2.1 Island formation

There are different hypotheses about the formation of the East Frisian Islands. The theory of Barckhausen (1969) implies that the barrier islands were formed by the dynamics of currents, swell and wind (Streif, 1990). They developed from periodically flooded sand flats into barrier beaches that were partially unaffected by high tides, towards dune islands, representing the final stage of development. This process was initiated 3000 years ago and still continues (Pott, 2003). According to Streif (1990, 2002), a Pleistocene core was identified at 5-10 m depth below the southwestern part of Spiekeroog, which formed the substratum on which Holocene coastal sediments accumulated.

2.2 Geomorphological development of the Ostplate

Until approximately 1860, Spiekeroog had a length of 6 km. Only in the following decades the island grew to its present extent of 9.8 km (Sindowski, 1973). According to Röper et al. (2013), the development of the Ostplate from a periodically flooded sand flat to a dune island started around 1940, the first dunes appearing in the 1970s. On the basis of aerial pictures, Röper et al. (2013) identified three stages of dune formation:

In 1938, the Ostplate was characterized by a continuous sand flat without any dunes. Eckel (1977) reported an initial growth of dunes in the 1940s due to aeolian processes aggregating sediment above Mean High Water (MHW), but these small pioneer dunes were very unstable.

The second stage of dune formation was evoked by the occurrence of *Elymus farctus* (sand couch-grass). When the dunes reached a height of 1 m above MHW (i.e. 2.39 m above sea level (asl)) around 1960 (Röper et al., 2013), *E. farctus* was able to spread extensively and caused further sediment accumulation up to 3 m asl (Eckel, 1977). As a result, the Ostplate was characterized by a thin foredune ridge with a height of 3 m asl in 1985 (Röper et al., 2013). The growth of the dunes led to a change in vegetation.

Around 1970, *Ammophila arenaria* (European beachgrass) appeared for the first time and started to displace the former dominating species *E. farctus* (Eckel, 1977). According to Petersen and Pott (2005), the spreading of *A. arenaria* corresponds to the formation of white dunes. The presence of *A. arenaria* indicates a freshening process, since *A. arenaria* requires, in contrast to *E. farctus*, a salinity of $< 1 \text{ g l}^{-1}$ (Eckel, 1977; Petersen and Pott, 2005). Due to its capability to capture aeolian sediments, dunes were able to grow further (Streif, 1990), leading to a maximum dune height of 9 m asl in 1999 and approximately 11 m asl in 2011, still mainly characterized as white dunes but in some areas also as grey dunes (Röper et al., 2013). The shelter of the dunes also enabled the tidal flat to rise continuously above MHW, resulting in the extensive growth of salt marshes (Röper et al., 2013). These salt marshes, located in the supralittoral and flooded episodically, exhibit a characteristic zonation of vegetation ranging from pioneer marsh to upper salt marsh vegetation (Petersen and Pott, 2005).

2.3 Hydrology and hydrogeology

The East Frisian Islands, including Spiekeroog, are affected by semidiurnal tides (Liebscher and Baumgartner, 1996). With a mean tidal range of 2.72 m, the tidal regime of Spiekeroog can be classified as mesotidal (Hayes, 1979; Federal Waterways and Shipping

Administration [WSV], 2016). MHW reaches 1.39 m asl and Mean Low Water (MLW) 1.33 m below sea level (bsl; annual means from 1995 to 2015, WSV, 2016). The mean spring range and the mean neap range is 3.09 m and 2.23 m, respectively (Federal Maritime and Hydrographic Agency [BSH], 2017, pers. comm.; WSV, 2016). In the two years prior to sampling, five storm tides were recorded reaching a maximum height of 3.64 m asl. A storm tide is defined as a tide that reaches > 1.5 m above MHW (i.e. > 2.89 m asl) and a storm tide is classified as “heavy” when it reaches > 2.5 m above MHW (i.e. > 3.89 m asl), which occurred last in December 2013 (high tide: 4.14 m asl, WSV, 2016, Fig. 2).

Spiekeroog has a temperate climate with all-season rainfall. The average annual precipitation amounts to 808 mm (from 1984 to 2011, OOWV, 2012). Dune islands like Spiekeroog exhibit almost no surface run-off in dune areas due to the high permeability of the sands. As a result, fresh groundwater recharge occurs in the dunes (Streif, 1990). Based on apparent ^3H - ^3He ages, Röper et al. (2012) calculated a mean groundwater recharge rate of 300-400 mm a^{-1} in the dunes. However, due to the less permeable fine grained sediments of the marsh (clay and silt) as well as the existence of tidal creeks, recharge rates are much lower in the marsh (Wiederhold et al., 2015). The freshwater lens in the western part of Spiekeroog has a thickness of ~44 m and is used for the island’s public water supply (Röper et al., 2012). Until recently, little to no information on the existence of freshwater below the Ostplate was available. Röper et al. (2013) were the first to carry out pore water samplings along several profiles at the Ostplate in 2011 and 2012, and measured water table salinities. Results proved the existence of freshwater on the Ostplate in a narrow zone below the dunes surrounded by brackish water (Röper et al., 2013). Due to the frequent inundation of the salt marsh covering most of the southern area of the Ostplate and the beach to the North, brackish to saline groundwater prevailed in these areas.

3. Material and methods

In order to investigate the spatial and temporal variations of the extent of the freshwater lens below the Ostplate, the electrical conductivity of shallow pore water (near the

water table) was measured and ground surface elevation recorded. In combination with information on storm surge and tidal water levels obtained from the nearest tide gauges, these data were analyzed with regard to the correlation between ground surface elevation, inundation frequency and water table salinity. Laser-scan elevation models of 1999, 2008 and 2014 (provided by the Lower Saxony Water Management, Coastal Defence and Nature Conservation Agency [NLWKN]) were used to identify areas of the Ostplate affected during the respective (storm) tides. The most current laser-scan elevation model together with a biotope map of 2004 (provided by the Wadden Sea National Park of Lower Saxony administration [NLPV]) was used to investigate whether or not a relationship between vegetation zonation, ground surface elevation and water table salinity exists.

3.1 Sampling

Pore water measurements in the area of the dunes at the Ostplate were conducted to determine the boundary between shallow fresh- and brackish groundwater (at a salinity of 1 g l⁻¹, Fig. 1). Horizontal positions of the pore water sampling points were located with a GPS (Etrex 20, Garmin) in the area of the dunes. In addition, pore water measurements were carried out along three north-south oriented profiles (P1-P3, Fig. 1) to locate the freshwater-saltwater interface. Sampling took place in November 2015 (296 sampling points), February 2016 (254 sampling points) and September 2016 (433 sampling points). Horizontal and vertical positions of the sampling points along the three profiles were determined with a differential GPS (Leica SR530, accuracy of 2 cm). In situ pore water sampling and measurements of electrical conductivity were conducted with stainless steel tubes of up to 2 m length and a sampling window (length of filter screen) between 4 and 5.5 cm at the bottom (see Röper et al., 2013). To reach the saturated zone, the tubes were pushed into the ground as deep as possible to depths of up to 1 m in marsh areas and up to 2 m below ground surface elevation in dune and beach areas (see supplementary material Table I). The pore water was extracted by suction with a 60 ml syringe. To verify extraction out of the saturated zone, i.e. groundwater, it was ensured that the pore water was bubble-free. The electrical

conductivity was immediately measured with a Hach HQ 40d multi device (automatic temperature correction to 25 °C) and was converted into salinity using the method of Stuyfzand (1993):

$$\text{Salinity} = f * EC_{25} \quad (1)$$

where EC_{25} is the electrical conductivity ($\mu\text{S cm}^{-1}$) of the water at 25 °C and f is a conversion factor. However, the original factor of Stuyfzand (1993) was slightly modified based on measurements of electrical conductivity and total dissolved solids of 25 groundwater samples from the Ostplate, and was calculated as $f = 0.6768$. Freshwater, brackish water and saltwater were classified according to Freeze and Cherry (1979) and have a salinity of <1, 1 to 10 and >10 (g l^{-1}), respectively.

3.2 Inundation frequency

The frequency of flooding at the sampling points along the three profiles was determined for the year prior to the respective date of sampling. This was achieved using water level data from two tide gauges located southwest of Spiekeroog (average distance to the study site: 7 km; WSV, 2016) and southwest of Wangerooge (average distance to the study site: 6 km; WSV, 2016) were analyzed (Fig. 2). Together with the elevation of the sampling points, this information enabled an estimation of the inundation frequency at each respective sampling point.

Fig. 2

3.3 Map construction

A laser-scan elevation model of 2014 (provided by the NLWKN) with a resolution of 1 m (square grid) and a density of laser dots of three points per m^2 was used to differentiate between flooded and non-flooded areas of the Ostplate during (storm) tides with various

water levels (Fig. 2). We focused on the highest water level in the year prior to each sampling campaign (Fig. 2). For the sampling campaign in November 2015, the highest preceding water level was 3.64 m asl (301 days before sampling), while for the February and September 2016 campaigns the highest preceding water level was 3.15 m asl (84 and 280 days before sampling, respectively).

In order to create past and present areal salinity maps of the Ostplate, the derived empirical equation was applied to laser-scan elevation models of 2014, 2008 and 1999 (provided by the NLWKN) using ArcGIS. The laser-scan elevation models of 2008 and 2014 were also used to gather information on the morphological changes over time (i.e. net sedimentation or erosion) in the study area by subtraction of the two grids in ArcGIS. To investigate the relationship between vegetation zonation (particularly within the salt marsh), ground surface elevation and water table salinities, the constructed water table salinity map of 2014 was overlain with a biotope map (provided by the NLPV). An aerial image of 2013 (provided by the NLWKN) was used as a background for various maps.

4. Results and discussion

4.1 Spatial extent and temporal variability of the shallow freshwater

Maps of measured water table salinity for November 2015 (Fig. 3 A), February 2016 (Fig. 3 B) and September 2016 (Fig. 3 C) show a decrease in water table salinities towards the dunes where the ground surface elevation increases. The existence of freshwater (salinities $< 1 \text{ g l}^{-1}$) below the entire dune ridge is in agreement with Röper et al. (2013). The freshwater is surrounded by brackish groundwater (salinities between 1 and 10 g l^{-1}). With increasing distance from the dunes towards the MHW-line in the north as well as in the south, increasing salinities were observed (Fig. 3). In all three measuring campaigns, the highest salinities were detected beneath the MHW-line in the pioneer marsh in the south ($\sim 34 \text{ g l}^{-1}$) and at the beach in the north ($\sim 32 \text{ g l}^{-1}$), which resemble the salinity of the North Sea ($\sim 34 \text{ g l}^{-1}$). The sampling point density was much greater (see 3.1) than in Röper et al. (2013, about 167 sampling points in total) and suggests one continuous freshwater lens below the

dunes in the eastern part of the Ostplate, which exhibit the longest continuous dune ridge. In contrast, several smaller separated lenses below the dunes in the western part of the Ostplate become visible in Fig. 3. According to Houben et al. (2014), who likewise found separate lenses on the adjacent island of Langeoog, the existence of separate freshwater lenses is mainly caused by overwash events during storm tides. In combination with the information on flooded and non-flooded areas, results show that the mapped shallow boundary between fresh- and brackish water is located roughly at the boundary between flooded and non-flooded areas, i.e. the dune base (Fig. 3).

However, the agreement between elevated areas not flooded during the highest preceding storm tides and presence of freshwater is less pronounced in November 2015 and September 2016, especially in the eastern part of the Ostplate (Fig. 3 A, C). At various sampling points, the distance between the freshwater boundary and the non-flooded areas is several tens of meters, especially towards the beach. In contrast, in February 2016 the boundary between fresh- and brackish water was detected almost exactly at the elevation of the highest preceding storm tide (2015/11/30, colored in Fig. 3 B). This suggests that the time between sampling in autumn (10 months) and late summer (9 months) and the last storm tides which flooded the entire Ostplate except the areas colored in green in the previous winter (2015/01/11; Fig. 3 A) and in the previous autumn (2015/11/30, light blue colored; Fig 3 B, C), was sufficient to cause some degree of freshening and expansion of the shallow freshwater, especially towards the permeable beach.

Fig. 3

The comparison of the three campaigns (Fig. 3) suggests temporal variations of the spatial extent of the freshwater lenses. At least near the surface, the freshwater lenses had the largest extent in November 2015 and September 2016, i.e. after/during a summer without storm flood events, while the area underlain by freshwater shrank in February 2016, following a winter with several storm floods. Based on the 1 g l^{-1} contour line, the shrinkage is $\sim 18\%$.

Hence, storm tides and resulting inundations just before the measurements in February 2016 led to a salinization of the freshwater lens at its fringes. Likewise, over the summer period, the transition zone between fresh- and saltwater moved seawards and areas north of the dunes in particular (sandy areas) were freshened, a pattern already suggested by Röper et al. (2013). According to Houben et al. (2014), localised run-off from the dune top to the nearest dune valley leads to focused infiltration at the dune base, probably due to the water repellency of dry dune sands. This observation may explain the visible freshening in this area. Houben et al. (2014) calculated recharge rates of 400 mm a^{-1} for the dune valleys of Langeoog, which corresponds to findings of Röper et al. (2012) on Spiekeroog and Post and Houben (2017) on Baltrum. Other authors also reported a seaward movement of the interface between fresh- and saltwater during summer, caused by the absence of flood events in combination with fast rainwater recharge through the permeable sands (Michael et al., 2005; Terry and Falkland, 2009; Villholth et al., 2005). Naturally, higher recharge rates would enhance the freshening, whereas more evapotranspiration leads to a decreased recharge, resulting in higher water table salinities. An influence of fresh groundwater discharge on the water table salinities near the dunes is unlikely, since numerical modelling showed that fresh groundwater discharge occurs approximately at the MLW-line (Röper et al., 2013).

According to Fig. 3, the time passed since the last inundation clearly affects water table salinity. In an attempt to further explore this dependency, water table salinities were plotted versus the time passed since the last flooding with seawater at each respective point in time (see supplementary material Fig. I). Freshwater was encountered where the last inundation occurred 7-10 months or more prior to sampling (~302-303 days in November 2015 and ~219 days and ~280 days, respectively in September 2016) for locations showing freshwater ($<1 \text{ g l}^{-1}$). This is similar to findings by Terry and Falkland (2009) who reported a recovery time of 11 months for salinized shallow freshwater. The short recovery time of one sampling location in February 2016 (~84 d) is however surprising. The fast recovery of the water table salinities is probably not only the result of vertical flow due to recharge by rainfall,

but also due to density-driven vertical flow (saltwater fingers), as suspected by Buddemeier and Oberdorfer (2004) and suggested by simulations of Post and Houben (2017). The scattering in Fig. 1 is large, probably due to the fact that only three sampling campaigns were conducted. For example, there are many sampling locations where the time period passed since the last inundation was similarly short to that at the freshwater locations, yet brackish water was encountered. Furthermore, there was a wide range of salinities measured at locations that were flooded on the day prior to sampling, ranging from ~ 11 to 35 g l^{-1} . Generally, lower salinities were encountered in the upper salt marsh, while higher salinities were encountered in the lower salt marsh and pioneer zone with a lower ground surface elevation. This shows that the frequency of flooding (see below) is a better indicator for water table salinity than the time passed since the last inundation.

4.2 Dependence of water table salinities on inundation frequency and ground surface elevation

The salinity near the water table depends on the frequency of inundation, which in turn depends on the ground surface elevation as well as on the sea level. Freshwater was only found at sites below the dunes that were flooded three times or less in the year before sampling (Fig. 4). Generally, if sampling points were flooded more often, the shallow groundwater was brackish, similar to observations by Terry and Falkland (2009) for groundwater at an atoll island in the South Pacific Ocean. When inundated, a non-linear rise of salinity was recorded (Fig. 4). At low inundation frequencies, the rise in salinity was steeper, i.e. only a few additional inundations already led to saltwater salinities ($> 10 \text{ g l}^{-1}$). This strong impact of a small number of inundations on groundwater salinities was also observed by Klaassen et al. (2008) for a sand bar in the North Sea (Kachelotplate) and applies until approximately 70 floodings per year. At higher inundation frequencies, the gradient decreases. Maximum salinities (about 34 g l^{-1}) were encountered beneath the MHW-line at the pioneer marsh, subject to 565 (November 2015) and 587 (February 2016).

inundations within the preceding year. The dependence of water table salinity, Sal_{GW} [g l⁻¹] on inundation frequency, ω [1/a] can be described by the following logarithmic equation:

$$Sal_{GW} = a_1 \ln(\omega) + b_1 \quad (2)$$

where ω is the number of inundations in the year prior to sampling, a_1 is 4.85 and b_1 is -0.047, as results of a non-linear least square fitting analysis (data points: 120, $R^2 = 0.89$, lower confidence interval (CI) of a_1 : 4.54, upper CI of a_1 : 5.16; lower CI of b_1 : -1.22, upper CI of b_1 : 1.12). This relationship between salinity and inundation frequency may be transferable to other tidally influenced islands or coastal environments with a similar hydrogeological setting. However, the applicability at other sites should be tested in further studies. Note that only profiles P1-P3 were considered in Fig. 4 and for equation 2 because the ground surface elevation at these points was measured with great precision at the time of sampling. For the remaining profiles, only the digital elevation map of 2014 was available.

Fig. 4

To validate the accuracy of equation 2, measured versus calculated salinities were plotted. The comparison of the calculated salinity values with the measured ones shows a fairly good correlation ($R^2 = 0.87$, see supplementary material Fig. II).

Naturally, the frequency of inundation depends on the ground surface elevation. The relationship between ground surface elevation [m asl] and inundation frequency is curvilinear (Fig. 5 A): with increasing elevation, the frequency of inundation decreases. At heights greater than 3 m asl (at the edge of the dunes), sampling points were not flooded or flooded only once, i.e. only during the highest storm tide within the previous year. At ground surface elevations above 2 m asl, relatively few inundations were recorded and the frequencies changed slowly with rising ground surface elevation. The gradient is steepest at a ground surface elevation between 1 and 2 m asl, where a small change in ground surface elevation results in a rapid change in inundation frequency. At a ground surface elevation of 1 m asl, flooding occurs twice daily.

Fig. 5

The relation between ground surface elevation and salinity is shown in Fig. 5 (B). With decreasing ground surface elevation, the salinity increases. Beneath MHW, no further increase of salinity with decreasing elevation occurs, as seawater salinities are already reached. Ignoring the low-lying areas (Fig. 5 B) that are exposed to daily flooding (points tagged with a red circle), the dependence of water table salinity, Sal_{GW} [g l⁻¹] on ground surface elevation, h [m asl] can be described by the following exponential equation:

$$Sal_{GW} = a_2 e^{(b_2 h^2)} \quad (3)$$

where h is the ground surface elevation [m asl], and a_2 is 57.51 and b_2 is -0.320 as results of a non-linear least square fitting analysis (data points: 115, $R^2 = 0.85$, lower CI of a_2 : 50.44, upper CI of a_2 : 64.58; lower CI of b_2 : 0.28, upper CI of b_2 : 0.36). Although some data scattering and a wide salinity range in lower-lying areas is visible, the trend is obvious and the relationship is described reasonably well with the exponential function. Thereby it is seemingly irrelevant whether or not a sampling point is located north or south of the dunes (i.e. on the permeable beach or within the marsh covered by impermeable sediments). Both Fig. 4 and Fig. 5 (B) suggest that other factors (e.g. recharge, evapotranspiration), which of course have influence on the salinity, are of less importance. If these factors were of greater importance for the water table salinity, the scattering in both figures would also be greater. Though somewhat trivial and rather intuitive, the dependence of groundwater salinity on ground surface elevation in the inundation fringe has, at least to our knowledge, previously not been quantified in a similar manner. It has yet to be tested whether or not the relationship between ground surface elevation and water table salinity can be transferred to other islands or coastal environments with a similar mean tidal range.

4.4 Extrapolation and reconstruction of present and past water table salinities depending on ground surface elevation

Present water table salinities for the entire study area were extrapolated based on equation 3 and ground level information from 2014 (Fig. 6 A). Salinities of 34.11 g l^{-1} (highest salinities measured) were assigned to areas located $< 1.39 \text{ m asl}$ (MHW-line). Fig. 6 A visualizes the resulting predicted spatial groundwater salinity distribution. Water table salinity decreases from the MHW-line inland towards the more elevated dunes underlain by freshwater, following a gradient perpendicular to the coastline. This pattern was also observed in salt marshes described by Sánchez et al. (1998).

Fig. 6

Based on equation 3 and elevation data of the study area of 1999 and 2008 (laser-scan elevation models of 1999 and 2008, provided by the NLWKN), water table salinities were also reconstructed for those years and illustrated as past water table salinity maps (Fig. 6 C, B). Overall, the maps indicate decreasing water table salinities within the salt marsh between 1999 and 2014 (Fig. 6 A-C, Table 1). The figures also illustrate an expansion in width of areas underlain by freshwater with time. Based on the salinity maps (Fig. 6 A-C) the areas underlain by freshwater covered 0.34 km^2 in 2014 compared to 0.29 km^2 in 2008 and 0.24 km^2 in 1999. Since the laser-scan elevation model of 1999 had a much lower resolution and partial errors, it is probably less reliable than the models of 2008 and 2014. However, with dune growth (Fig. 6 D), the size of the freshwater lenses has clearly increased over the past 15 years. Equation 3 assumes no change in mean sea level over time, which is reasonable given the short period of time. A significant change of the hydrological boundaries (e.g. mean sea level, mean tidal range) would, however, modify equation 3 severely.

Equation 3 was derived from ground surface elevation and water table salinities of all three profiles. To check its validity, measured water table salinities of the sampling points were plotted versus calculated salinities derived from equation 3. The comparison of the calculated salinity values with the measured ones shows a fairly good correlation ($R^2 = 0.85$, see supplementary material Fig. III). In addition, we calculated equations with values of two profiles only and adapted the resulting equations to the third profile in each case (for the comparison of the calculated salinity values with the measured ones see supplementary material Table II).

Table 1: Areas [km^2] underlain by brackish- ($1\text{-}10 \text{ g l}^{-1}$) and saltwater ($> 10 \text{ g l}^{-1}$) and their changes in area size over time (1999-2014).

Year	$1\text{-}5 \text{ g l}^{-1}$	$5\text{-}10 \text{ g l}^{-1}$	$10\text{-}20 \text{ g l}^{-1}$	$20\text{-}30 \text{ g l}^{-1}$
2014	0.42	0.43	1.90	3.33
2008	0.32	0.40	1.92	3.38
1999	0.33	0.37	2.14	3.24

Given the causal relationship between ground surface elevation and water table salinity, salinity changes from 1999 to 2014 must have inevitably been caused by rising elevations following net sedimentation. Fig. 6 D gives information on net increases or decreases of the ground surface elevation in the study area for the time period between 2008 and 2014. A similar pattern is likely for the time period from 1999 to 2008, but the laser-scan model of 1999 does not allow for such an analysis. However, Röper et al. (2013) documented a continuous growth of the entire Ostplate and in particular of the dunes since the 1940s based on analysis of aerial photographs. Since 2008 (Fig. 6 D), the elevation related to MHW has changed by vertical accretion within the salt marsh. Giani et al. (2003) investigated sedimentation rates at the western part of Spiekeroog and found mean sedimentation rates of $\sim 0.2\text{-}0.5 \text{ cm a}^{-1}$ by analyzing the vertical Cs-137 distribution. In foreland salt marshes at the mainland, sedimentation rates of approximately 1 cm a^{-1} were reported (Giani et al., 1994). Based on our results, we expect water table salinities to

continue to decrease in future, following the general growth trend of the Ostplate. Consequently, areas underlain with freshwater will also continue to grow.

Based on numerical modelling, the total volume of the freshwater lenses below the Ostplate was estimated to be around 42-92 million m³ by Röper et al. (2013). This figure is only an estimate, as long as the vertical extent of the freshwater lenses are not yet known. Preliminary data of observation wells installed recently along profile P1 indicate a maximum thickness of approximately 4 – 5 m. The simulation did, however, clearly show that the freshwater lenses have not yet reached a steady state and that the size of the freshwater lenses will continue to grow for another 300-500 years. This can be assumed to be even more so, as the dunes themselves continue to grow, which was disregarded in the simulations by Röper et al. (2013). However, continuous freshening depends on the amount of freshwater recharge and inundation frequencies evoked by storm tides, whereby the latter will be affected by future seawater levels (Klaassen et al., 2008; Sulzbacher et al., 2012).

The freshening will also depend on the type and density of dune vegetation affecting transpiration rates. Given that the mean sea level is expected to rise in the southern North Sea as an effect of climate change (IPCC, 2007), the relative velocities of sedimentation and sea-level rise will determine whether or not the observed freshening trend will continue. Eitner (1996), however, predicted a growth of barrier islands like Spiekeroog with rising sea levels given a sufficient supply of sediment and accommodation space, which would dampen the effect of rising sea levels and storm frequencies on water table salinities.

4.5 Relationship between ground surface elevation, inundation frequency, water table salinity and vegetation

Overall, the distribution of biotope types reflects the water table salinity distribution below, with salinities > 30 g l⁻¹ corresponding generally to the pioneer marsh and the lower beach near the MHW-line, 20-30 g l⁻¹ to the lower salt marsh (and the central beach), 5-20 g l⁻¹ to the upper salt marsh (and the upper beach) and < 5 g l⁻¹ to the dunes (Fig. 7). Sánchez et al. (1998) also observed salinity decreases with increasing distance from the shore in salt

marshes. This is not surprising, as both are mainly a function of inundation frequency, itself being a function of ground surface elevation as exemplified above. Suchrow and Jensen (2010) reported that the elevation gradient is linked to salinity in foreland salt marshes along Germany's North Sea coast; salinity in turn reflects changes in the composition of species along the elevation gradient, which is also visible in Fig. 7. Hence, in the absence of digital ground surface models and groundwater data, one could also infer water table salinities from biotope maps, as water table salinities are somewhat more difficult to obtain with instrumentation only.

Fig. 7

The cross sections in Fig. 8 show the ground surface elevation of the profiles P1-P3 from north to south together with the vegetation zones along the profiles. The heights corresponding to the inundation frequencies of the vegetation zones given by Erchinger (1985) were extracted from Fig. 5 A, and the measured water table salinities (with information on the depth from which samples were taken, sampling campaign November 2015) are additionally depicted. These cross sections containing the measured salinities verify the correspondence between vegetation zonation and water table salinities, which in turn depends on ground surface elevation and with that inundation frequency as suggested (Fig. 5). This is in accordance with the findings of Suchrow and Jensen (2010), although, in the study presented here, vegetation zones (i.e. biotope types) were considered instead of individual species.

With regard to the relation between inundation and biotope types that were found at the sampling locations, the recorded frequency of 111-145 inundations in the lower salt marsh (marked in dark green color) as well as the recorded frequency of 10-85 inundations in the upper salt marsh (marked in light green color) are in accordance with Erchinger (1985; Fig. 5 A). Likewise, the measured ground surface elevation of the sampling points inside the lower and upper salt marsh conform with those of Preising et al. (1990; lower salt marsh: 0-20 cm above MHW, upper salt marsh: 20-40 cm above MHW), with few exceptions. The

recorded frequency of inundations for the pioneer marsh (108-565, marked in brown color) is less than the frequency given by Erchinger (1985), who suggested 400-700 inundations per year, following investigations of vegetation zonation in salt marshes of the Wadden Sea. According to Preising et al. (1990), the pioneer marsh in Lower Saxony is located between 40 cm below MHW and MHW while most of the sampling points classified as pioneer marsh on the Ostplate lie above MHW (Fig. 5 A, Fig. 8), which explains the lower inundation frequency. One possible explanation may be the duration of each inundation, which might also effect pioneer marsh vegetation. In contrast to other parts of the study area, this site might exhibit less drainage and therefore longer exposure to seawater, resulting in higher salinities. However, as few sampling points were located in the pioneer marsh, further investigations are necessary to clarify this discrepancy.

A restriction of our analysis is that the vegetation was only considered at biotope level. Following studies should be scaled down to species distribution, similar to the investigation of Suchrow and Jensen (2010).

Fig. 8

5. Conclusions

This study provides an overview of the impacts of storm tides and inundation frequency on water table salinities below an evolving barrier island that is subject to tides and winter storm surges and remains largely unaffected by anthropogenic activities. The following conclusions can be made:

1. The near surface extent of the shallow freshwater is largely determined by storm tides and shows spatial and temporal variations. Winter storm tides with high water levels cause shrinkage, whereas the absence of storm tides accompanied by groundwater recharge during the summer months leads to a recovery and an increase in the area

underlain by freshwater. The role of density-driven flow is unclear and should be considered in future investigations.

2. In an area with a given tidal range, the ground surface elevation determines the inundation frequency which in turn influences the water table salinity. If flooded more than three times in the previous year, brackish groundwater is present in the shallow subsurface. The lower the ground surface elevation of an area, the higher the inundation frequency and the higher the water table salinity.
3. The dependence of the water table salinity on the inundation frequency can be quantified with a logarithmic function, whereas the dependence of the water table salinity on the ground surface elevation can be quantified with an exponential function, which appears to be independent of the sediment type encountered (i.e. sand on the beach and in the dunes versus clay and silt in the marsh).
4. The inundation frequency is a better predictor of water table salinity than the time since the last inundation.
5. In conjunction with digital elevation models, the exponential function allows calculations of past and present water table salinities on barrier islands as a consequence of changing ground surface elevation in a highly active environment in terms of morphodynamics. The method is useful with respect to generating numerical models on freshwater lens formation, allowing to estimate former (and future) salt input due to flooding, and is potentially also applicable to other barrier islands. Therefore, we suggest to test the method at different sites affected by tides and storm surges to verify its application.
6. The identified match between water table salinities and vegetation zones suggest that water table salinities may be inferred from often more easily accessible vegetation zone maps.
7. The vertical extent of the freshwater lens as well as the variability of salinity at different depths will be the subject of future studies. Multi-level observation wells installed along profile P 1 will be used to calculate and predict the present and future

volume of the freshwater lens on the Ostplate. Furthermore, well data will provide more information about how (storm) tides influence the freshwater lens.

Acknowledgements

The authors wish to thank the Nationalparkverwaltung Niedersächsisches Wattenmeer (NLPV), especially Gerald Millat and Claus Schulz for giving us the possibility to conduct studies on the Ostplate. Many thanks to the Niedersächsischer Landesbetrieb für Wasserwirtschaft, Küsten- und Naturschutz (NLWKN), mainly Holger Dirks and Rabea Tants, for providing the laser-scan elevation models and the aerial image. We thank the Wasser- und Schifffahrtsverwaltung des Bundes (WSV) and the Bundesamt für Seeschifffahrt und Hydrographie (BSH) for providing data of the tide gauges. Many thanks to Leon Diehl, Tomas Fresenborg, Felix Grünenbaum, Tobias Haene, Alina Harms, Johanna Kleinschnitker and Sebastian Schäfer for their support in sampling. We would also like to thank Udo Uebel for the GPS-data analysis and Charlotte Winkelmann and Swaantje Fock from the Nationalparkhaus Wittbülten at Spiekeroog for their logistical support. We are grateful to Wencke Appel, Julia Bell and Rosanna Schöneich-Argent for proofreading. We thank three anonymous reviewers and Adrian Werner for their helpful comments and advices for improving the manuscript. We also thank the German Research Foundation for project funding (DFG project number MA 3274/6-1).

References

- Anderson Jr, W.P., 2002. Aquifer salinization from storm overwash. *Journal of Coastal Research* 18 (3), 413–420.
- Anderson Jr., W.P., Lauer, R.M., 2008. The role of overwash in the evolution of mixing zone morphology within barrier islands. *Hydrogeology Journal* 16 (8), 1483–1495.
- Barckhausen, J., 1969. Entstehung und Entwicklung der Insel Langeoog-Beiträge zur Quartärgeologie und Paläogeographie eines ostfriesischen Küstenabschnittes-Oldenburger Jb., 68: 239-281 (in German).

- Bockelmann, A.-C., Bakker, J.P., Neuhaus, R., Lage, J., 2002. The relation between vegetation zonation, elevation and inundation frequency in a Wadden Sea salt marsh. *Aquatic Botany* 73 (3), 211–221.
- Bockelmann, A.-C., Neuhaus, R., 1999. Competitive exclusion of *Elymus athericus* from a high-stress habitat in a European salt marsh. *Journal of Ecology* 87 (3), 503–513.
- BSH (Bundesamt für Seeschiffahrt und Hydrographie), 2017. Mean neap tide data at Tide Gauge Spiekeroog 2016.
- Buddemeier, R.W., Oberdorfer, J.A., 2004. Hydrogeology of Enewetak Atoll, Geology and Hydrogeology of Carbonate Islands. Elsevier, pp. 667–692.
- Collins III, W.H., Easley, D.H., 1999. Fresh-water lens formation in an unconfined barrier island aquifer. *Journal of the American Water Resources Association* 35 (1), 1–22.
- Eckel, H., 1977. Studien zur morphologischen Entwicklung der Ostplate Spiekeroogs. Dissertation. Westfälischer Wilhelms-Universität Münster (in German).
- Eitner, V., 1996. Geomorphological response of the East Frisian barrier islands to sea-level rise: an investigation of past and future evolution. *Geomorphology* 15 (1), 57–65.
- Erchinger, H.F., 1985. Dünen, Watt und Salzwiesen. Das Niedersächsische Ministerium für Ernährung, Landwirtschaft und Forsten, Hannover, 1–59 (in German).
- Fetter, C.W., 1972. Position of the saline water interface beneath oceanic islands. *Water Resources Research* 8 (5), 1307–1315.
- Freeze, R.A., Cherry, J.A., 1979. Groundwater. Prentice Hall, Englewood Cliffs, N.J.
- Giani, L., Ahrens, V., Duntze, O., Irmer, S.K., 2003. Geo-pedogenesis of salic fluvisols on the North Sea island of Spiekeroog. *Journal of Plant Nutrition and Soil Science* 166 (3), 370–378 (in German).
- Giani, L., Henken, R., Schröder, H., 1994. Schwermetallanreicherungen in Salzmarschen der südlichen Nordseeküste. *Journal of Plant Nutrition and Soil Science* 157 (4), 259–264 (in German).

- Gingerich, S.B., Voss, C.I., Johnson, A.G., 2017. Seawater-flooding events and impact on freshwater lenses of low-lying islands. Controlling factors, basic management and mitigation. *Journal of Hydrology* (2017), <http://dx.doi.org/10.1016/j.jhydrol.2017.03.001>.
- Hayes, M.O., 1979. Barrier island morphology as a function of tidal and wave regime. In: Leatherman, S.P. (Ed.), *Barrier Islands*. Academic, New York.
- Houben, G.J., Koeniger, P., Sültenfuß, J., 2014. Freshwater lenses as archive of climate, groundwater recharge, and hydrochemical evolution. Insights from depth-specific water isotope analysis and age determination on the island of Langeoog, Germany. *Water Resources Research* 50 (10), 8227–8239.
- IPCC 2007. In: Solomon, S., Qin, D., Manning, M., Chen, Z., Marquis, M., Averyt, K.B., Tignor, M., Miller, H.L., (Eds.), 2007. Contribution of Working Group I to the Fourth Assessment Report of the Intergovernmental Panel on Climate Change. Cambridge University Press, Cambridge, United Kingdom and New York. Accessed.
- Klaassen, K., Bormann, H., Klenke, T., Liebezeit, G., 2008. The impact of hydrodynamics and texture on the infiltration of rain and marine waters into sand bank island sediments - Aspects of infiltration and groundwater dynamics. *Senckenbergiana maritima* 38 (2), 163–171.
- Klassen, J., Allen, D.M., 2017. Assessing the risk of saltwater intrusion in coastal aquifers. *Journal of Hydrology* (2017), <http://dx.doi.org/10.1016/j.jhydrol.2017.02.044>.
- Liebscher, H.-J., Baumgartner, A., 1996. *Allgemeine Hydrologie, Quantitative Hydrologie*. Gebrüder Borntraeger, Berlin-Stuttgart (in German).
- Michael, H.A., Mulligan, A.E., Harvey, C.F., 2005. Seasonal oscillations in water exchange between aquifers and the coastal ocean. *Nature* 436 (7054), 1145–1148.
- NLPV (Nationalparkverwaltung Niedersächsisches Wattenmeer). Biotope map after TMAP-code of 2004.
- NLWKN (Niedersächsischer Landesbetrieb für Wasserwirtschaft, Küsten- und Naturschutz). Laser-scan elevation models of 1999, 2008 and 2014, aerial image of 2013.

OOVV (Oldenburgisch-Ostfriesischer Wasserverband), 2012. Precipitation and Lysimeter

Data of Spiekeroog Island from 1984-2011.

Petersen, J., Pott, R., 2005. Ostfriesische Inseln: Landschaft und Vegetation im Wandel. Schlütersche, Hannover (in German).

Post, V.E.A., Houben, G.J., 2017. Density-driven vertical transport of saltwater through the freshwater lens on the island of Baltrum (Germany) following the 1962 storm flood. *Journal of Hydrology* (2017), <http://dx.doi.org/10.1016/j.jhydrol.2017.02.007>.

Post, V.E.A., 2005. Fresh and saline groundwater interaction in coastal aquifers. Is our technology ready for the problems ahead? *Hydrogeology Journal* 13 (1), 120–123.

Pott, R., 2003. Die Nordsee: Eine Natur-und Kulturgeschichte. CH Beck, München (in German).

Preising, E., Vahle, H.C., Brandes, D., Hofmeister, H., Tüxen, J., Weber, H.E., 1990. Die Pflanzengesellschaften Niedersachsens – Bestandsentwicklung, Gefährdung und Schutzprobleme, Wasser-und Sumpfgesellschaften des Süßwassers. Naturschutz Landschaftspflege Nds (20/8) (in German).

Robinson, C., Li, L., Prommer, H., 2007. Tide-induced recirculation across the aquifer-ocean interface. *Water Resources Research* 43 (7), W07428.

Röper, T., Greskowiak, J., Freund, H., Massmann, G., 2013. Freshwater lens formation below juvenile dunes on a barrier island (Spiekeroog, Northwest Germany). *Estuarine, Coastal and Shelf Science* 121-122, 40–50.

Röper, T., Kröger, K.F., Meyer, H., Sültenfuss, J., Greskowiak, J., Massmann, G., 2012. Groundwater ages, recharge conditions and hydrochemical evolution of a barrier island freshwater lens (Spiekeroog, Northern Germany). *Journal of Hydrology* 454-455, 173–186.

Sánchez, J.M., Izco, J., Medrano, M., 1996. Relationships between vegetation zonation and altitude in a salt-marsh system in northwest Spain. *Journal of Vegetation Science* 7 (5), 695–702.

- Sánchez, J.M., Otero, X.L., Izco, J., 1998. Relationships between vegetation and environmental characteristics in a salt-marsh system on the coast of Northwest Spain. *Plant Ecology* 136 (1), 1–8.
- Schneider, J.C., Kruse, S.E., 2006. Assessing selected natural and anthropogenic impacts on freshwater lens morphology on small barrier Islands. Dog Island and St. George Island, Florida, USA. *Hydrogeology Journal* 14 (1-2), 131–145.
- Silvestri, S., Defina, A., Marani, M., 2005. Tidal regime, salinity and salt marsh plant zonation. *Estuarine, Coastal and Shelf Science* 62 (1-2), 119–130.
- Sindowski, K.-H., 1973. Das ostfriesische Küstengebiet. Inseln, Watten und Marschen. Borntraeger, Berlin u.a. (in German).
- Streif, H., 1990. Das ostfriesische Küstengebiet. Nordsee, Inseln, Watten und Marschen; mit 10 Tabellen. Borntraeger, Berlin-Stuttgart (in German).
- Streif, H., 2002. The Pleistocene and Holocene Development of the Southeastern North Sea Basin and Adjacent Coastal Areas. In: G. Wefer, W.H. Berger, K.-E. Behre, E. Jansen (Editors), *Climate Development and History of the North Atlantic Realm*. Springer Berlin Heidelberg, Berlin, Heidelberg, s.l., pp. 387–397.
- Stuyfzand, P.J., 1993. Hydrochemistry and hydrology of the coastal dune area of the Western Netherlands. Zugl.: Amsterdam, Univ., Diss., 1993. KIWA, Nieuwegein.
- Suchrow, S., Jensen, K., 2010. Plant Species Responses to an Elevational Gradient in German North Sea Salt Marshes. *Wetlands* 30 (4), 735–746.
- Sulzbacher, H., Wiederhold, H., Siemon, B., Grinat, M., Igel, J., Burschil, T., Günther, T., Hinsby, K., 2012. Numerical modelling of climate change impacts on freshwater lenses on the North Sea Island of Borkum using hydrological and geophysical methods. *Hydrology and Earth System Sciences* 16 (10), 3621–3643.
- Terry, J.P., Falkland, A.C., 2009. Responses of atoll freshwater lenses to storm-surge overwash in the Northern Cook Islands. *Hydrogeology Journal* 18 (3), 749–759.
- Vacher, H.L., 1988. Dupuit-Ghyben-Herzberg analysis of strip-island lenses. *Geological Society of America Bulletin* 100 (4), 580–591.

- Vandenbohede, A., Lebbe, L., 2007. Effects of tides on a sloping shore. Groundwater dynamics and propagation of the tidal wave. *Hydrogeology Journal* 15 (4), 645–658.
- Villholth, K.G., Amerasinghe, P.H., Jeyakumar, P., Panabokke, C.R., Woolley, O., Weerasinghe, M.D., Amalraj, N., Prathepaan, S., Bürgi, N., Sarath Lionel Rathne, D.M., 2005. Tsunami impacts on shallow groundwater and associated water supply on the East Coast of Sri Lanka. Report from the International Water Management Institute, Colombo, Sri Lanka.
- Werner, A.D., Bakker, M., Post, V.E., Vandenbohede, A., Lu, C., Ataie-Ashtiani, B., Simmons, C.T., Barry, D.A., 2013. Seawater intrusion processes, investigation and management. Recent advances and future challenges. *Advances in Water Resources* 51, 3–26.
- White, I., Falkland, T., 2010. Management of freshwater lenses on small Pacific islands. *Hydrogeology Journal* 18 (1), 227–246.
- White, I., Falkland, T., Perez, P., Dray, A., Metutera, T., Metai, E., Overmars, M., 2007. Challenges in freshwater management in low coral atolls. *Journal of Cleaner Production* 15 (16), 1522–1528.
- Wiederhold, H., Scheer, W., Sulzbacher, H., Siemon, B., Kirsch, R., 2015. Nordseeinseln im Klimawandel—die Nordfriesische Insel Föhr und die Ostfriesische Insel Borkum. Aktuelle Küstenforschung an der Nordsee. *Coastline Reports* 25 (2015), 45–48 (in German).
- Wolner, C.W., Moore, L.J., Young, D.R., Brantley, S.T., Bissett, S.N., McBride, R.A., 2013. Ecomorphodynamic feedbacks and barrier island response to disturbance. Insights from the Virginia Barrier Islands, Mid-Atlantic Bight, USA. *Geomorphology* 199, 115–128.
- WSV (Wasser- und Schifffahrtsverwaltung des Bundes), 2016. High and Low Water Data at Tide Gauge Spiekeroog and Wangerooge 1995–2016 and mean spring tide data at Tide Gauge Spiekeroog 2016. Provided by Bundesanstalt für Gewässerkunde (BfG).
- Yang, J., Graf, T., Herold, M., Ptak, T., 2013. Modelling the effects of tides and storm surges on coastal aquifers using a coupled surface-subsurface approach. *Journal of Contaminant Hydrology* 149, 61–75.

Fig. 1: Map of the study area 'Ostplate', located at the eastern part of Spiekeroog, Northwest Germany. Pore water measurements were carried out at the marked profiles P1 – P3 and around the dune area. Aerial picture of 2013 provided by the NLWKN. Laser-scan elevation model of 2014 provided by the NLWKN.

Fig. 2: High-Tide-levels in the two years prior to sampling (data provided by WSV 2016). The highest water levels related to sampling in November 2015, February 2016 and September 2016 are marked. Following a failure of the tide gauge southwest of Spiekeroog on 2016/04/02, data of the tide gauge southwest of Wangerooge was used.

Fig. 3: Water table salinities in the areas surrounding the dunes and along the profiles P1-P3 in (A) November 2015, (B) February 2016 and (C) September 2016, plotted onto the aerial picture of 2013 (provided by the NLWKN). The areas of the Ostplate that were not flooded during storm tides with the highest water levels within the previous year before the sampling are colored and are restricted to the dune ridge. The Laser-scan elevation model of 2014 was provided by the NLWKN.

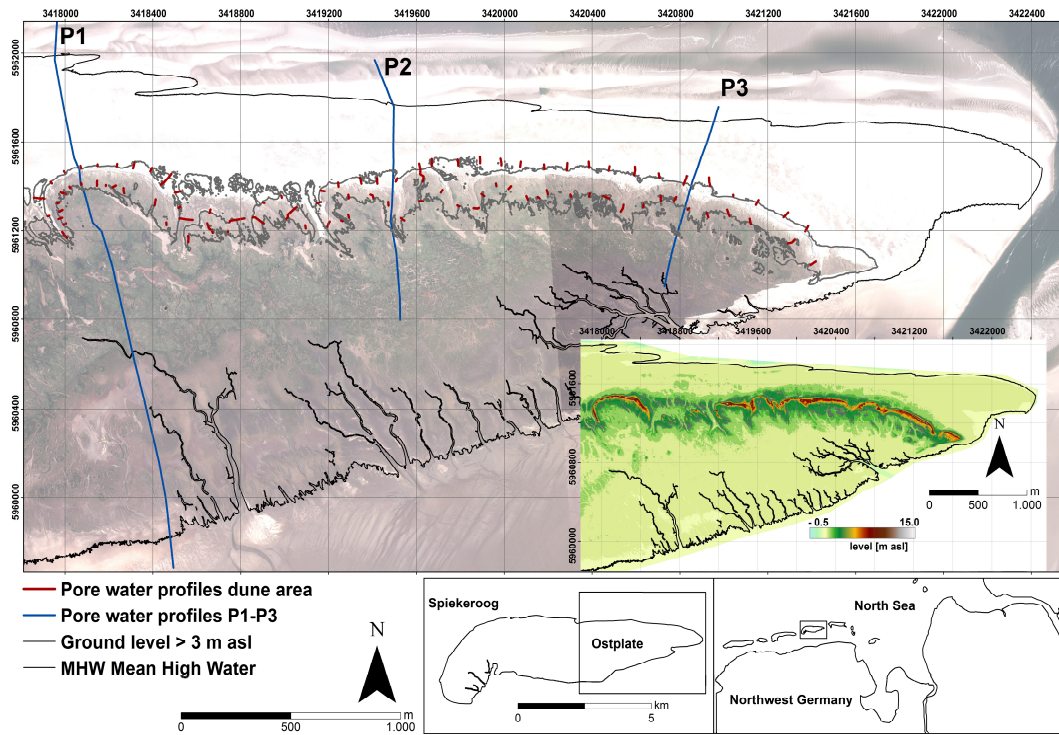
Fig. 4: Logarithmic relation between water table salinities along the profiles P1 – P3 in November 2015, February 2016 and September 2016 and inundation frequency at the sampling points within one year before sampling. The points tagged with a red circle (outliers) were not considered in creating the function $Sal_{GW} = 4.85\ln(\omega) - 0.047$ (A). Fig. 4 B displays an expanded view of the data points near the origin (0, 0) of Fig 4 A and shows the sampling points that were flooded up to 10 times within the previous year. The biotope types at the respective sampling points are indicated with a color code based on the biotope map of 2004 (provided by the NLPV).

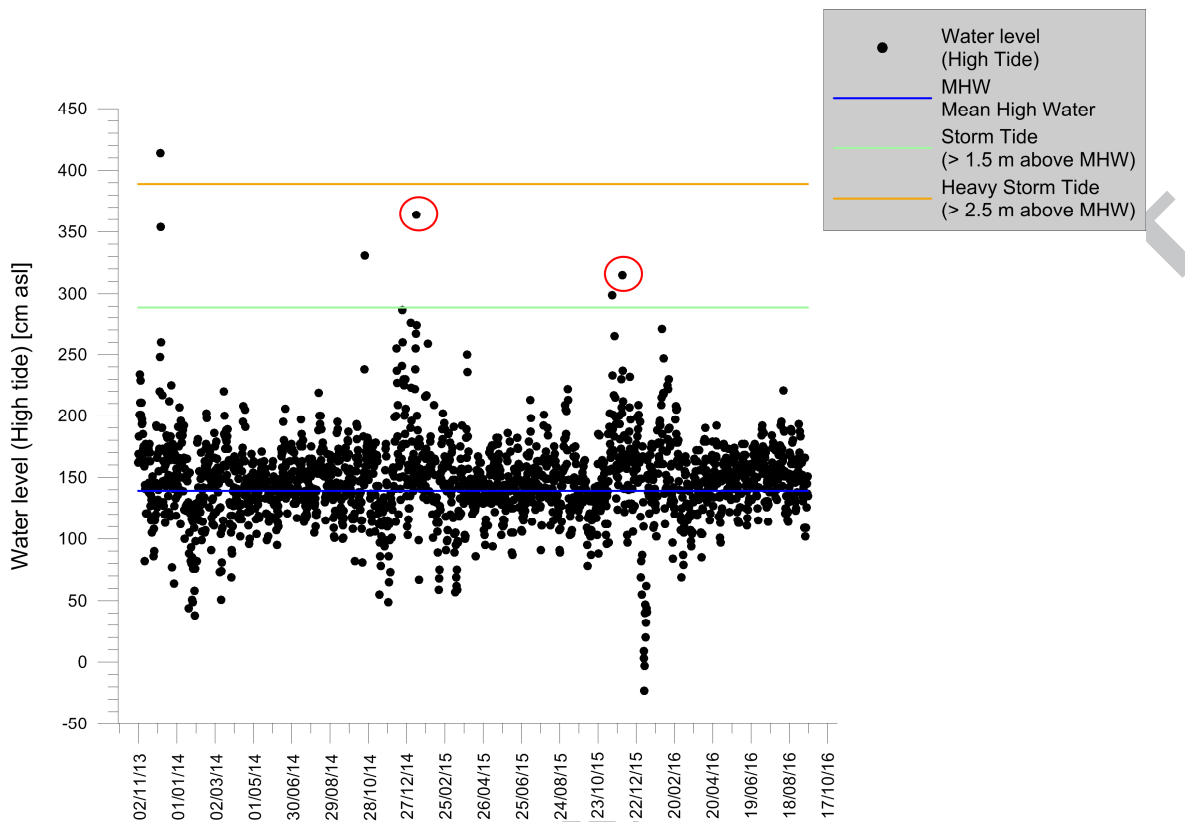
Fig. 5: (A) Number of inundations at the sampling points within one year before sampling depending on ground surface elevation [m asl] (November 2015, February and September 2016). Inundation frequencies in accordance to Erchinger (1985), who proposed 400-700 floodings per year for the pioneer marsh, 100-400 floodings for the lower salt marsh and 1-100 for the upper salt marsh, are plotted as dashed lines. (B) Exponential relation between groundwater salinities along the profiles P1 - P3 in November 2015, February and September 2016 and ground surface elevation above sea level at the sampling points. The points tagged with a red circle were not considered in creating the function $Sal_{GW} = 57.51e^{(-0.320h^2)}$ since these sampling points are located in low-lying areas which are exposed to daily floodings and seawater salinities are already reached. The height of MHW and Mean High Water Springs (MHWS) is also shown. The biotope types at the respective sampling points are indicated with a color code based on the biotope map of 2004 (provided by the NLPV).

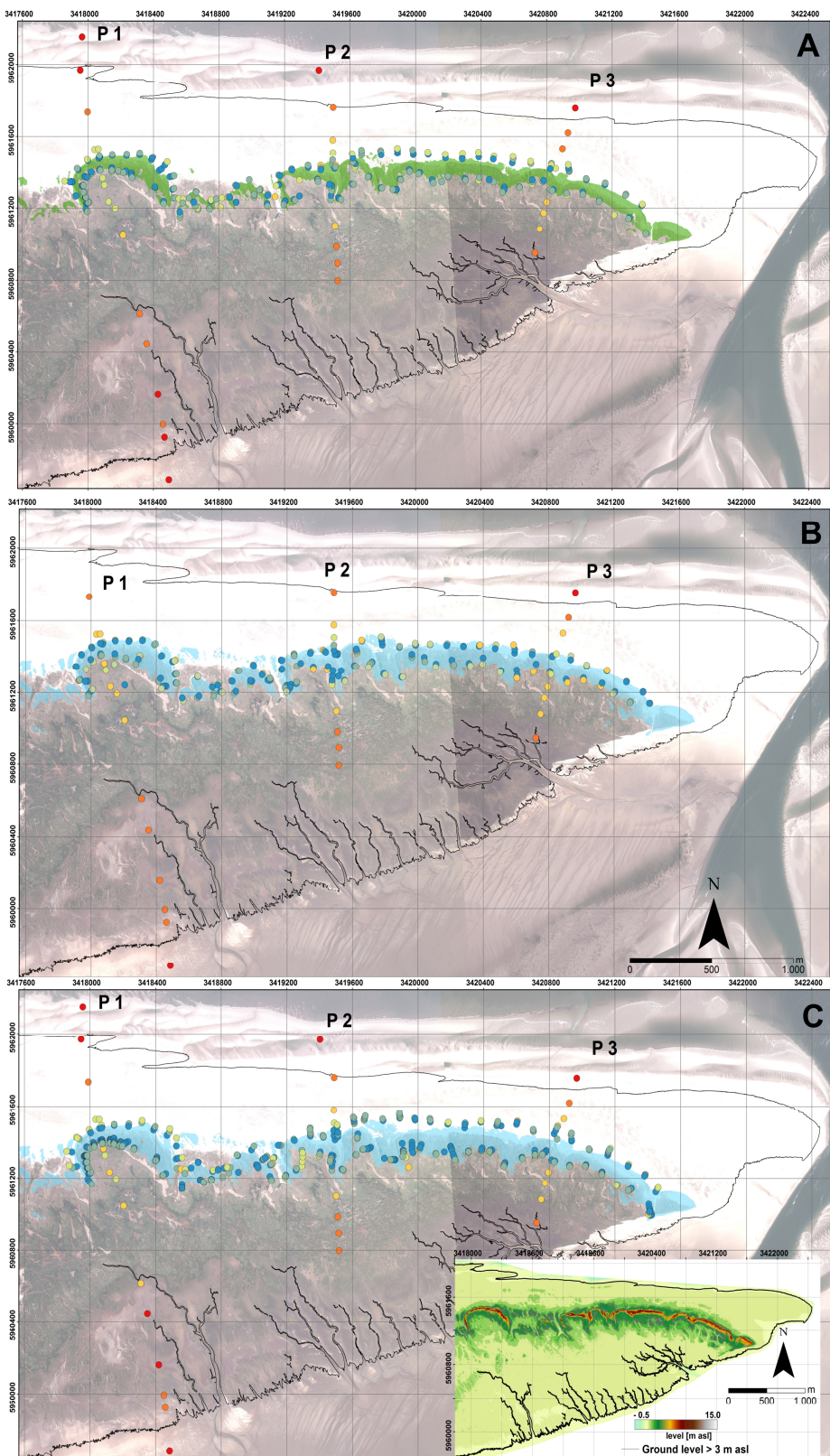
Fig. 6: Predicted water table salinities depending on ground surface elevation of (A) 2014, (B) 2008 and (C) 1999, based on the function $Sal_{GW} = 57.51e^{(-0.320h^2)}$. Laser-scan elevation models of 1999 and 2008 provided by the NLWKN. (D) Alteration of the ground surface elevation at the 'Ostplate' between 2008 and 2014. Ground surface elevations > 3 m asl are bordered grey. A ground surface elevation > 3 m asl represents the elevation where freshwater occurred (Fig. 5 B).

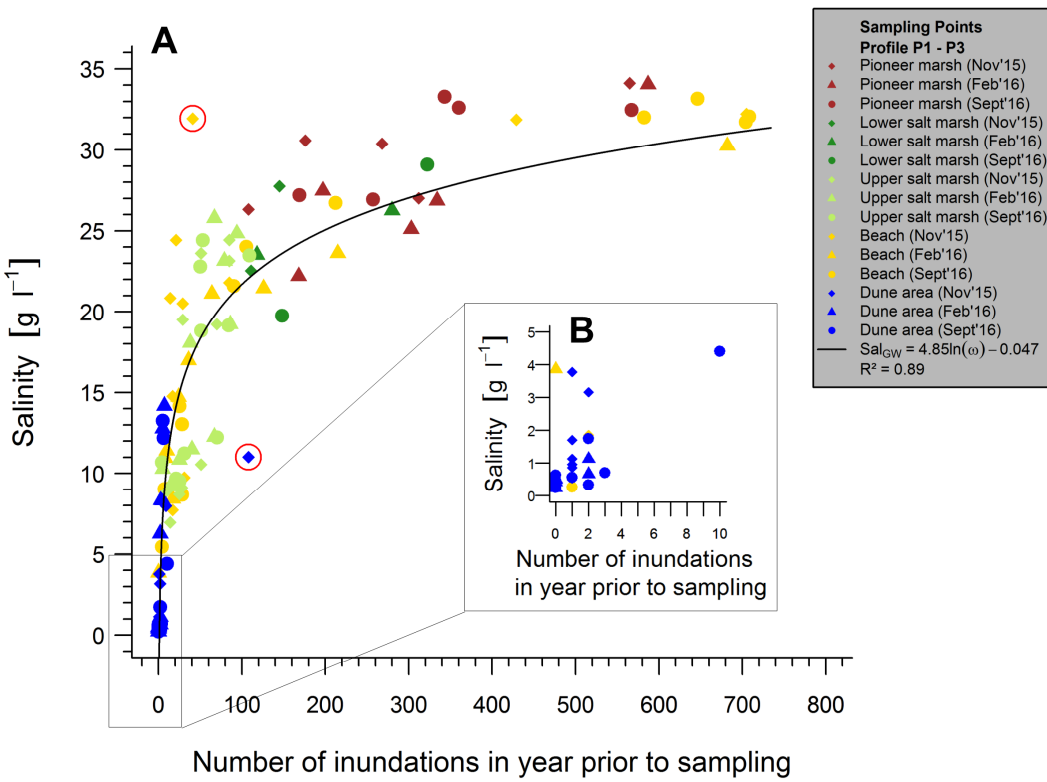
Fig. 7: Predicted water table salinities depending on ground surface elevation of 2014, based on the function $Sal_{GW} = 57.51e^{(-0.320h^2)}$. Vegetation zonation according to biotope type map of 2004 of the NLPV is also shown (**N**: North Sea, **B**: Beach, **D**: Dunes, **U**: Upper salt marsh, **L**: Lower salt marsh, **P**: Pioneer marsh, **T**: Tidal flat). Laser-scan elevation model of 2014 provided by the NLWKN.

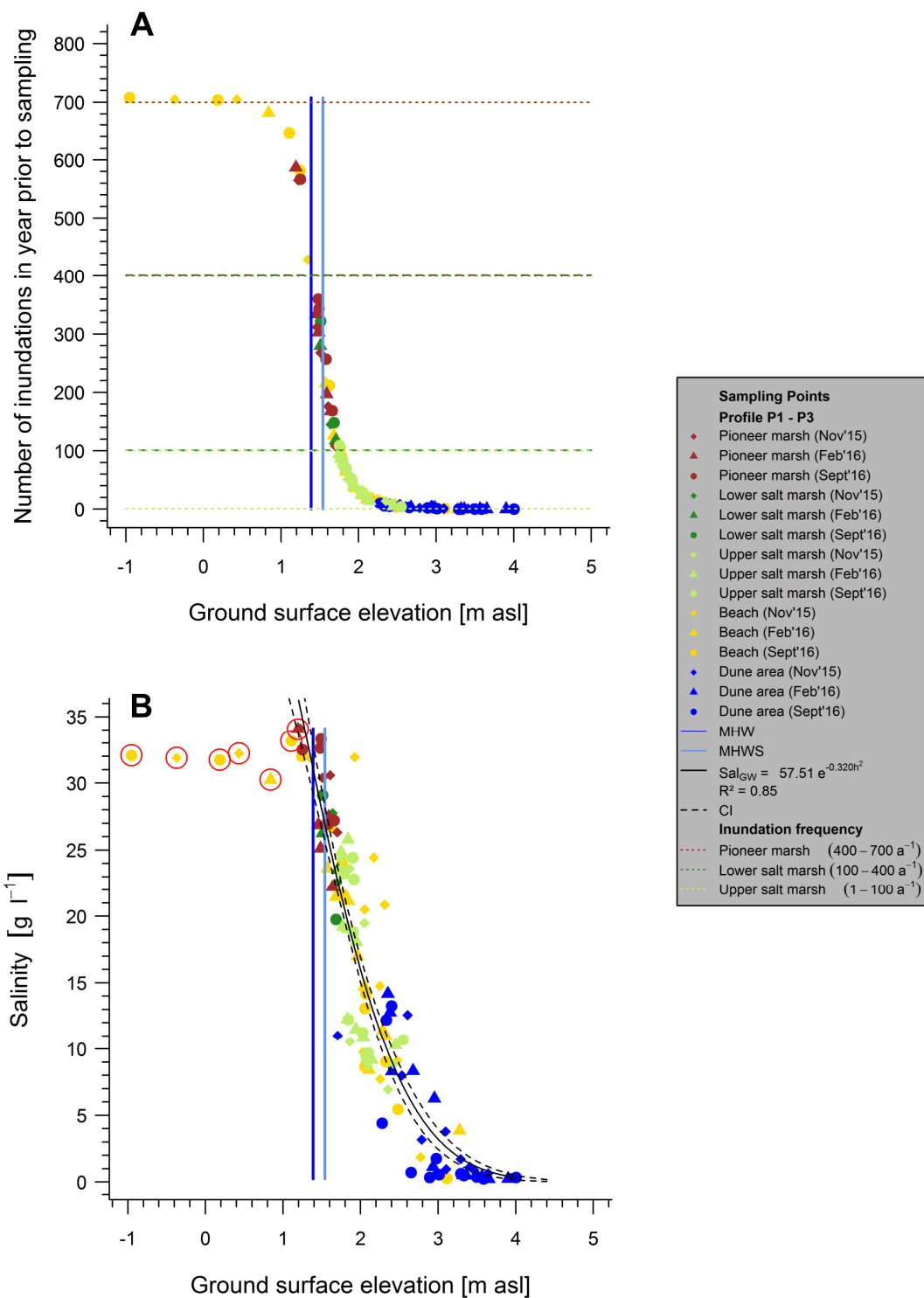
Fig. 8: Cross-sections of the profiles P1-P3 showing the ground surface elevation, water table salinities in the depth samples were taken (November 2015), vegetation zonation (NLPV, **N**: North Sea, **B**: Beach, **D**: Dunes, **U**: Upper salt marsh, **L**: Lower salt marsh, **P**: Pioneer marsh) marked with vertical lines and inundation frequency in accordance to Erchinger (1985) with distance from the MHW-line. The elevation of the highest water levels (compare Fig. 2 and Fig. 3) are also shown. On the right, measured ground surface elevation of the sampling points are plotted as a function of inundation frequency.

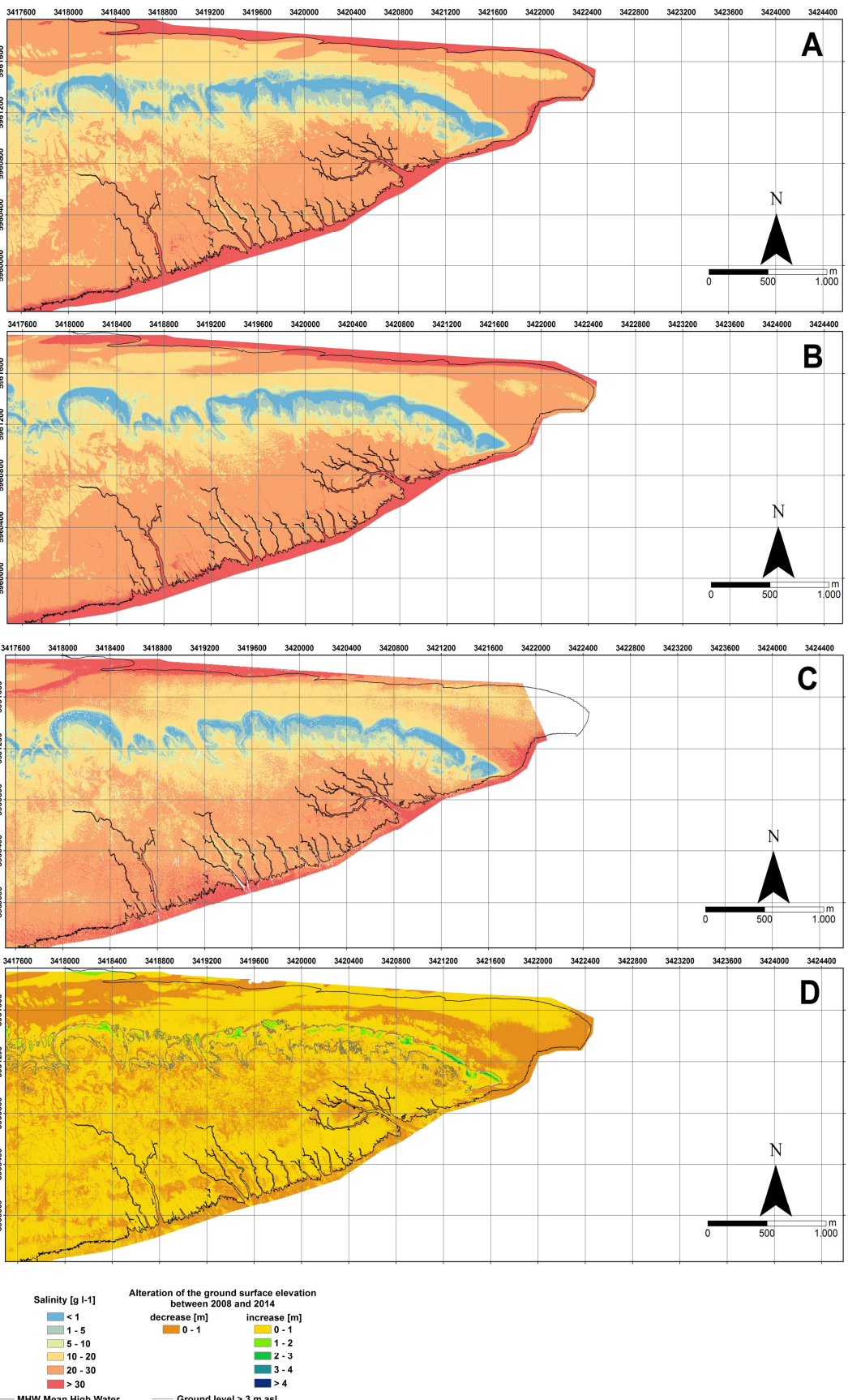




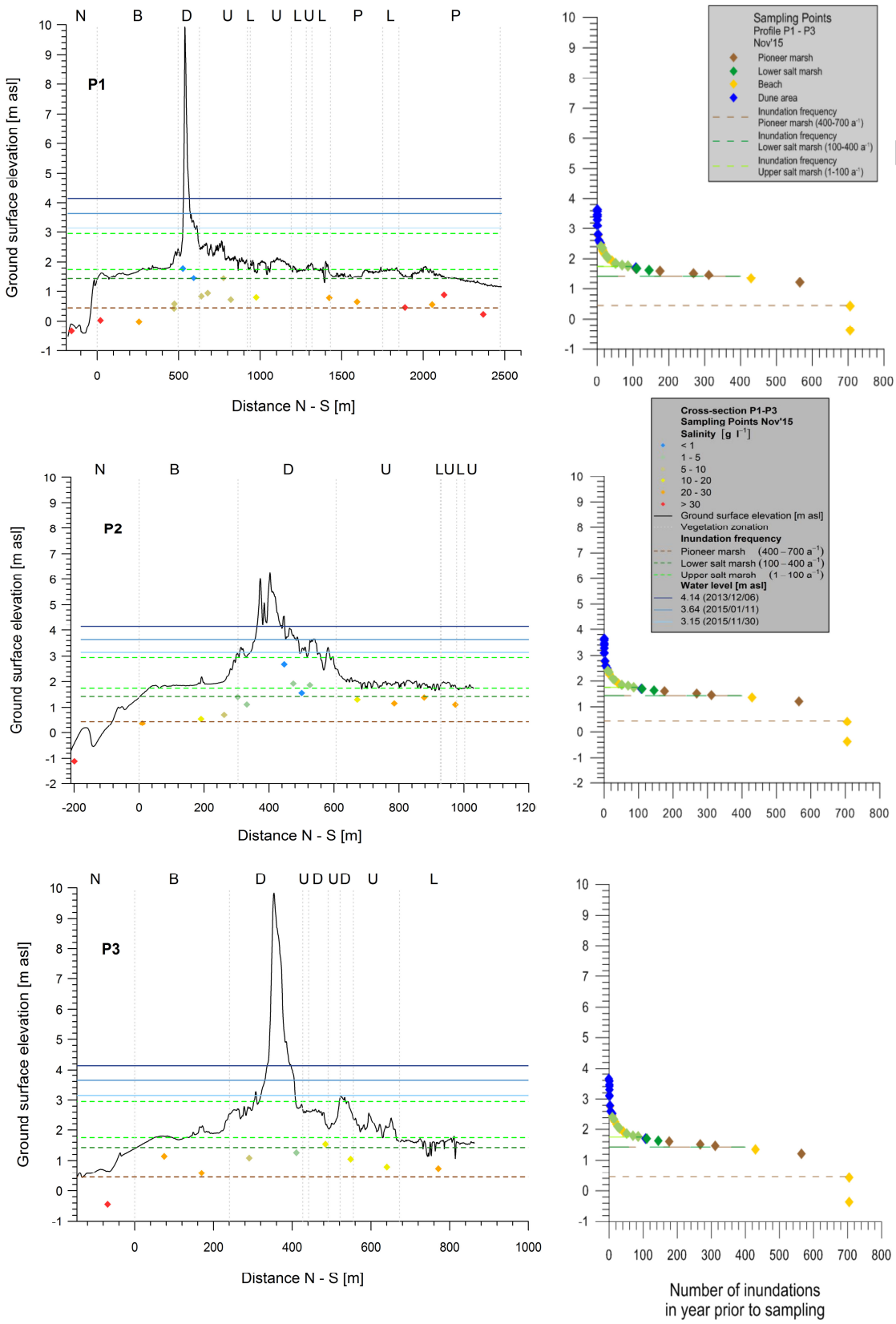












- Storm tides largely determine near surface extent of shallow fresh groundwater.
- Lower ground surface elevation results in higher inundation frequency and salinity.
- Function quantifies dependence of water table salinity on ground surface elevation.
- Water table salinities may be inferred from vegetation maps.

ACCEPTED MANUSCRIPT